Power improvement of the Stirling Amazon engine using modeling tools

Juan R. Vidal[1]
Vladimir M. Cobas[2]
Electo S. Lora[2]
Félix González[3]

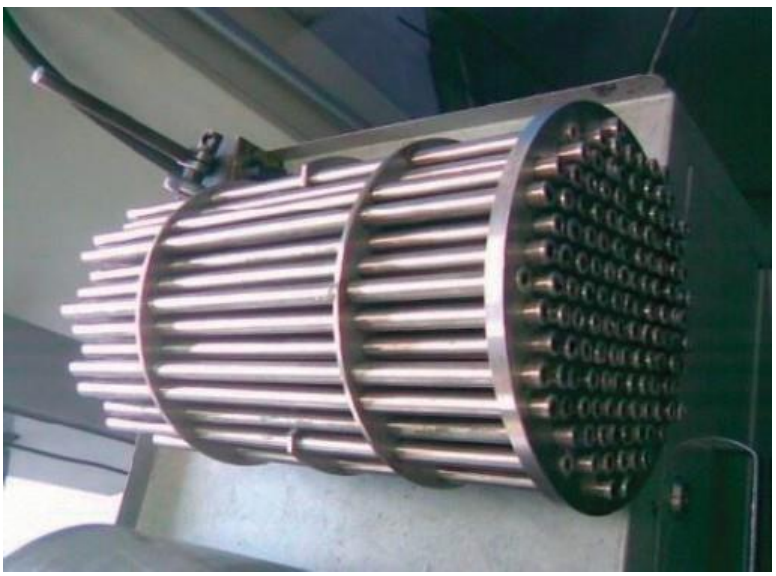

Abstract

Brazil has a great potential of biomass that can be used for electric generation. Furthermore, much of its territory is covered by forests, which are inhabited or have habitable regions, but face the problem of power shortages (Wilke & Silva, 2004). In this scenario, an alternative such as the Stirling engine is presented as a good way of energy supply in those isolated regions. This is the reason, the Excellency Group in Thermo-electric and Distributed Generation (NEST, for its acronym in Portuguese) at the Federal University of Itajubá, has designed a Stirling engine prototype to provide electricity to isolated regions of Brazil. This paper presents mathematical models of heat exchangers (hot, cold and regenerator) integrated into second order adiabatic models. The general model takes into account the pressure drop losses in the working fluids and exhaust gases, the thermal losses in the regenerator (not ideal), the hysteresis and losses due to internal heat transfer. The mathematical model, experimentally validated in the software PROSA ®, allowing improvements that increase the output power in the Amazon engine in 3,3 kW and reduce the dead volume to 7330 cm^3.

(1) Grupo de Investigación en Energías (GIEN). Universidad Autónoma de Occidente, Colombia.
Author to whom correspondence should be addressed. Electronic mail: jrvidal@uao.edu.co. Tel.: (55)3536291423.
(2) Núcleo de Excelência em Geração Termelétrica e Distribuída (NEST). Universidade Federal de Itajubá, Minas Gerais, Brasil.
(3) Centro de Estudios de Energía y Medio Ambiente (CEEMA). Universidad de Cienfuegos, Cuba.
Reception's date: 09/03/2016 – Aceptation's date: 22/05/2016.

Keywords: Stirling engine, mathematical modeling, biomass, distributed generation.

Resumen

Brasil tiene un gran potencial de la biomasa, el cual puede ser utilizado para la generación de electricidad. Además, gran parte de su territorio está cubierto por bosques, que están habitados o que tienen regiones habitables, pero se enfrentan al problema de la escasez de energía (Wilke & Silva, 2004). En este escenario, una alternativa como el motor Stirling se presenta como una buena opción para el suministro de energía en estas regiones aisladas. Por esta razón, el Núcleo de Excelencia en Generación Termo-Eléctrica y Distribuido (NEST), de la Universidad Federal de Itajubá, ha diseñado un prototipo de motor Stirling para proporcionar electricidad a las regiones aisladas de Brasil. Este artículo presenta los modelos matemáticos de los intercambiadores de calor (caliente, frío y regenerador) integrados en un modelo adiabático de segundo orden. El modelo general tiene en cuenta las pérdidas de caída de presión del fluido de trabajo y los gases de escape, así como las pérdidas térmicas en el regenerador (no ideal), la histéresis y las pérdidas debido a la transferencia de calor interna. Los resultados de este modelo matemático fueron comparados con los resultados del *software* PROSA ®, permitiendo mejoras que aumentan la potencia de salida del motor Amazonas en 3,3 kW y reducen el volumen muerto a 7330 cm^3.

Palabras clave: motor Sterling, modelado matemático, biomasa, generación distribuida.

Nomenclature

A	Area
A_{mr}	Surface area of the matrix
At	Cross-sectional area
C,m	Constants
C_{pg}	Specific heat of the working gas
D	Diameter
Dheh	Hydraulic diameter external horizontal
Diamt	Diameter of cold heat exchanger
h	Coefficient of heat transfer by convection
K	Thermal conductivity
L	Length
$\dot{m}$	Mass flow
Mec(2)	(1) - mechanical losses
M_{mr}	Mass mesh regenerative
m_w	Mesh Number
N	Number of tubes
nff	Number of rows in the cold heat exchanger
Nthptv	Number of horizontal tubes in vertical tube
Nu	Nusselt number
p	Loss, pressure
PCI	Calorific value of fuel
Pel	Electrical power
PotAdi(1)	Output power adiabatic model
Potsal	(6) - lost by hysteresis in the compression and expansion chambers.
PottNeta	Output Power (Potsal) - lost to outside pressure in the hot heat exchanger.
Pr	Prandtl number or pressure drop in the regenerator
$\dot{Q}$	Heat exchanged
Re	Reynolds Number
S	Perimeter of duct
St	Stanton Number
T	Temperature
Tcan(6)	(5) - lost by friction in the tubes of connectors of cold side.
Trc(4)	(3) - friction losses in the hot exchanger
Trf(3)	(2) - friction losses in the cold exchanger.
Trg(5)	(4) - friction losses in the regenerator
V	Velocity
$\dot{W}$	Output Power
γ	Specific heat relation
ρ	Density
η_{el}	Electrical efficiency
ω	Engine Velocity
ξ	Friction factor
Λ	Longitude reduced

Subscripts

Ac	Current engine
canal	connector tubes
crpp	Critical length of entry into a plane wall
ee	Exhaust Input
eef	Water Input
eh	External horizontal
en	Input to the engien
ev	External vertical
f	Referring to the cold heat exchanger
fc	Exhaust
ff	Water
h	Referring to the horizontal tubes, working gas in the hot heat exchanger or Hysteresis
hr	wire diameter in the regenerator
i	Ideal
iv	Internal vertical
k	Working gas in the cold heat exchanger
pe	Piston expansion
pp	Entry hydraulic to plane wall
r	Regenerator
s	Wall hot heat exchanger
sa	Output to the engine
se	Exhaust outlet
sef	Water output
sf	wall Cold heat exchanger
shutt	Shuttle
t	tubes
v	Referring to the vertical tubes
w	Wall

Introduction

At present, the Stirling machines are in commercial use as cooling machines, especially for cryogenic cooling and liquefaction of air. Although the technology of this engine is not fully developed, it has great potential to operate with high efficiency, fuel flexibility, low emissions, low noise, low vibration, and good performance at partial load (Aliabadi et al., 2009). The combination of biomass with a Stirling engine currently generates great interest to researchers and entrepreneurs, because biomass is considered a renewable energy source with the greatest potential to contribute in the energy needs of humanity (Bridgwater, 2003).

This paper studies the issues of modeling a Stirling Amazon engine designed by NEST to operate with biomass coming from the timber industry in Brazil. This engine is alpha type, with an initially designed generating capacity of 8 kW, and consists of five basic parts in its construction: the hot heat exchanger, the cold heat exchanger, the regenerator, the expansion chamber and the compression chamber, as well as the crank mechanism. This latter scheme, according to Cullen and McGovern (2010), is one of the main points of losses in Stirling engines. For this reason, the authors decided to use the crank mechanism of a motorcycle manufactured by Ducati in the Stirling Amazon engine.

Mathematical model of the Amazon Stirling engine

The mathematical model developed by the authors was coded in Visual Fortran ® and integrates models of heat exchangers, cold, hot, regenerating and secondary devices in the second order adiabatic model proposed by Urieli and Berchowitz (1984). Figure 1 shows the temperature distribution considered in the model and the system of generating.

Figure 1. a) Schematic model of the engine and b) The temperature distribution

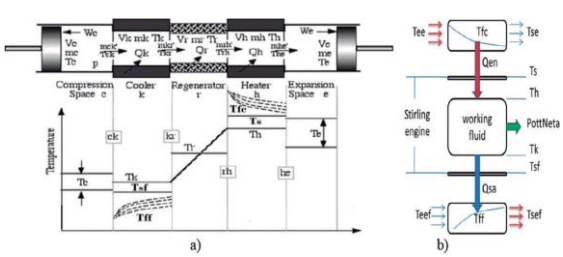

Source: by the author.

Mathematical model of hot heat exchangers

In the particular case of the Amazon engine, the hot heat exchanger has to exchange heat with the biomass furnace exhaust gases; this gas is a biphasic fluid (gas/solid or gas/liquid) that generates waste deposits in the external surfaces of the exchanger and significantly affects the engine efficiency (Kuosa, Kaikko & Koskelainen, 2007). In this framework, it may not have extended surfaces (like fins) (Podesser, 1999). It needs an induced draft fan to increase the convective heat transfer coefficient and cannot get their tubes in a cross flow as it would present a relative large fall of temperature. The fan also ensures the velocity of the exhaust gases and helps to overcome losses in heat exchangers by preheating the combustion air that is entering the furnace (Figure 2).

Figure 2. System of Stirling engine integrated with the biomass furnace

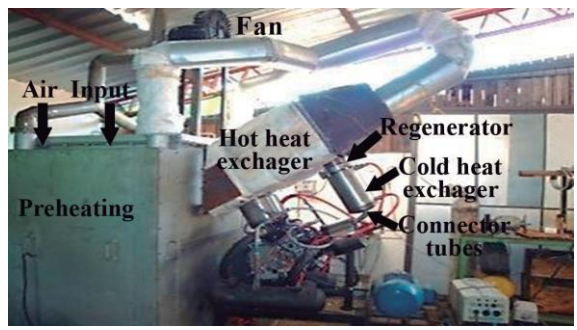

Source: by the author.

The outside of the heat exchanger is modeled in two parts, the first referred to the vertical tubes and the second to the horizontal tubes, getting the total heat delivered to the working fluid inside the exchanger (Figure 3).

The convective heat transfer coefficient (h_{ev}) in the vertical tubes on the outside is necessary to find the Nusselt number (Nu_{ev}) for a perpendicular flow to a bank of tubes using the following equation (Bergman, Lavine, Incropera & DeWitt, 1996).

$$Nu_{ev} = Fc\ C\ Re_{ev}^{m}\ Pr^{0.36}\left(\frac{Pr}{Pr_s}\right)^{\frac{1}{4}} \quad (1)$$

In the case of the exchanger studied, the Nusselt number has to be multiplied by a correction factor, Fc, since the number of rows is less than 20. The Reynolds number (Re_{ev}) is calculated with the maximum velocity (Vmax) that occurs between the outer surfaces of the vertical tubes.

Thus the convective heat transfer coefficient in the vertical tubes is:

$$h_{ev} = \frac{Nu_{ev} * K}{D_{ev}} \quad (2)$$

Figure 3. Hot heat exchanger

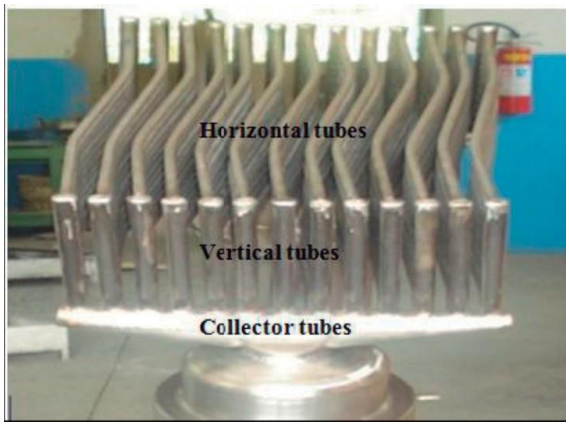

Source: by the author.

The calculation of the external heat transfer coefficient of horizontal tubes is done with the relationship of Nusselt number (Nu_{eh}) for parallel flow, where the Reynolds number (Re_{eh}) is calculated using the average velocity of the exhaust.

The horizontal tubes can be considered as flat walls. This is only valid when the boundary of the hydraulic layer does not exceed half the distance between the surfaces of adjacent tubes, if the overtaking happens; the behavior is as internal flow. Beyond these conditions, the analysis should be done considering a laminar or turbulent flow.

For the convective heat transfer coefficient inside the vertical tubes(h_{iv}), a cross-sectional area change is considered; this is due to the gradual incorporation of horizontal tubes along the vertical tubes that changes the velocity of the working fluid (V_{iv_i}).

$$V_{iv_i} = \frac{A_{pe} * V_{mpe}}{At_{iv} + \sum_0^n (i * At_{ih})} \quad (3)$$

With the variable velocity per stretch of the vertical tube, the Reynolds number (Re_{iv}) varies and therefore, the Nusselt number (Nu_{iv}) and the convective heat transfer coefficient (h_{iv}) vary too. In horizontal pipes, the relationship between Nusselt numbers is the same as on the inside of the vertical tubes.

Mathematical model of the cold heat exchanger

Likewise as for the hot heat exchanger (see Figure 4) , the analysis of the cold heat exchanger is made in two parts, the part on the outside which is the cooling water and the part on the inside which is the working gas.

To calculate the convective heat transfer coefficient on the outside of the tubes of this heat exchanger, the equation (1) for a bank of tubes was used, taking into account the number of steps in the shell. The same ratios that were used to calculate Nu_{iv} on the inner part of the hot heat exchanger are applied.

Figure 4. Cold heat exchanger

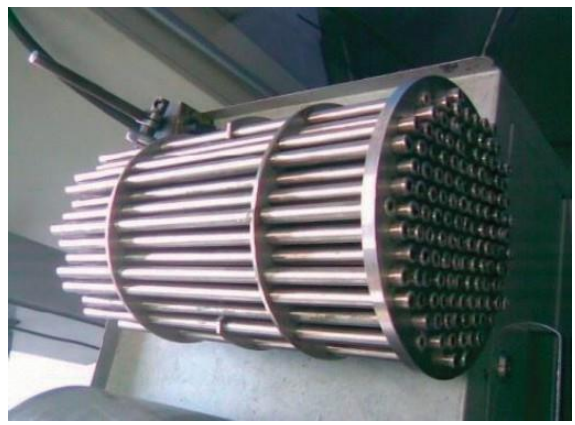

Source: by the author.

Calculation of the efficiency of regenerator

The calculations in the regenerator are made with the dimensionless parameters of Hausen (1929) which are improved in Hargreaves (1991), as shown in Table 1.

Table 1. Relations for the efficiency of regenerator (Hargreaves, 1991)

Re_r	Nu_r	h_r	Λ	Γ	Ω	η_r
$\frac{V_r\, Dhi}{\nu_r(1 - Dhi\, m_w)^2}$	$0.42Re_r^{0.56}$	$\frac{Nu_r K_r}{Dhi}$	$\frac{h_r A_{mr}}{\dot{m}C_{pg}}$	$\frac{M_{mr} C_M}{\dot{m}C_{pg}}$	$\frac{\Lambda}{\Gamma} + 2 - 2.35\left(\frac{\Lambda}{\Gamma}\right)^{\frac{1}{2}}$	$1 - \frac{2}{\Lambda + 2 - \Omega}$

Source: by the author.

Loss included in the model

The adiabatic model used needs to include the friction losses and heat transfer. The losses considered in this paper are:

• *Loss related to pressure drop* (Walker, 1980)

$$Pp = \sum \left[\frac{1}{\rho^2}\left(\frac{\dot{m}}{At}\right)^3 St\, L\, S\right] + \sum \left[\xi \frac{\rho}{2} At\, V^3\right] \quad (4)$$

• *Losses in the regenerator*

The pressure drop losses (equations 5) and thermal external losses (equations 7) considering the efficiency of the regenerator (Organ, 1997).

$$Pr = \left[\xi \frac{\rho}{2} At \frac{Lr}{2\,Dhi}\left[V\left(\frac{1}{1-Dhi\,\mathrm{m_w}}\right)^2\right]^3\right] \quad (5)$$

$$Qr = (1-\eta_r)Qre \quad (6)$$

• *Loss due to gas spring hysteresis*

For an ideal gas, the pressure/volume relationship is either isothermal or adiabatic. In a real gas, there is a certain amount of work that is dissipated (Timoumi, Tliliun & Nasrallahun, 2008). Urieli and Berchowitz (1984) propose the following expression.

$$Ph = \sqrt{\frac{1}{32}\omega\gamma^3(\gamma-1)T_w P\,K_w}\left(\frac{\Delta V}{V}\right)^2 A_w \quad (7)$$

• *Internal conductions*

Due to internal conduction between the hot parts and the cold parts of the engine through the different exchangers (Martini, 1983).

$$Qint = \frac{KA\Delta T}{L} \quad (8)$$

Where K is the thermal conductance of the material and A the effective area of conduction.

• *Shuttle conduction*

This happens for the expansion piston oscillation across a temperature gradient. It is usually not frequency-dependent for the speed and materials used in the engine. The piston absorbs heat during the hot end of its stroke and gives off heat during the cold end of its stoke (Lundqvist, 1993), as follows.

$$Qshutt = \frac{0.4E^2KgD\Delta T}{GLe} \quad (9)$$

Where E is the stroke of the piston, Kg is the thermal conductivity, D is the piston diameter, G clearance around the hot piston and L is the equivalent length of the piston.

• The pressure drop on the outside of the hot heat exchanger (in the exhaust gases).

$$\Delta Pv = NX\left(\frac{\rho Vmax^2}{2}\right)f \quad (10)$$

$$Pph = \sum\left[\frac{1}{\rho^2}\left(\frac{\dot{m}}{Ac}\right)^3 St\,L\,S\right]_{AR} \quad (11)$$

Where N is the number of rows of the heat exchanger and F and X are the friction and correction factors respectively.

• *Mechanical losses:*

Due to friction of piston rings, seals, bearings, sprockets and oil pumping (Thombare & Verma, 2008).

• *Pressure drop on the outside of the hot heat exchanger (in the exhaust gases)* (Bergman et al., 1996):

$$\Delta P = N_L f \chi \frac{\rho V_e^{\,2}}{2}$$

Where N is the number of rows of heat exchanger and F and X are the friction and correction factors respectively.

Method of solution

The system of differential equations of the adiabatic model was solved with the fourth order Runge-Kutta numerical method. The iterations in the adiabatic model end when they reach the allowed error given by the different values of initial temperature and final cycle. The equation (12) shows how to calculate the temperature of the working gas in the hot heat exchanger (Th). A similar relationship is used to calculate the surface of the cold heat exchanger.

$$Th = Ts - \frac{\dot{Q}_{en}}{h_h A_s} \quad (12)$$

The surface temperature of the wall of the heat exchanger (Ts) and the output temperature of the exhaust gas heat exchanger (Tse) are calculated with equations (13) and (14) respectively.

$$Tse = Ts - (Ts - Tee)\exp\left(\frac{-A_s h_{fc}}{\dot{m}_{fc} Cp_{fc}}\right) \quad (13)$$

$$\dot{Q}_{en} = \dot{m}_{fc} Cp_{fc}(Tee - Tse) \quad (14)$$

The use of equations (12), (13) and (14) require numerous iterations to try to stabilize the system, while reaching the predetermined errors. Thus, the only data required by the mathematical model are the temperatures and velocities of the exhaust gases and water that enters the heat exchangers, as well as the geometry of the engine,

the gas work and the efficiency of the mechanical and electrical generators.

Validation of the mathematical model

The comparison of results with the software PROSA (commercial Program for second order analysis) is shown in Figure 5.

Figure 5. Variation of efficiency and power output of the engine Amazon in function of RPM with the author´s model made (Efi and Potsal) and with the software PROSA (Efi PROSA and Pot PROSA)

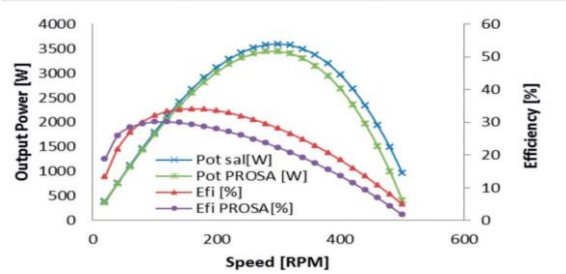

Source: by the author.

The PROSA was run under the same conditions that were used in the developed model. That is, in the hot heat exchanger dead volume of the collector tube was added, in the cold side the volume of the connecting tubes was added and wall temperatures were taken from the model proposed in this paper.

Results at Amazon Stirling engine

Characterization of losses

In the initial characterization the most significant pressure drops are presented in the order: the regenerator, the connector tubes of the cold side, hot and cold heat exchangers, and pressure drop in the outside heat exchanger, while the hysteresis losses are not significant. The losses in the connector tubes of the cold side are due to their low cross-sectional area (see Figure 6).

Figure 6. Initial characterization of pressure drop in the engine

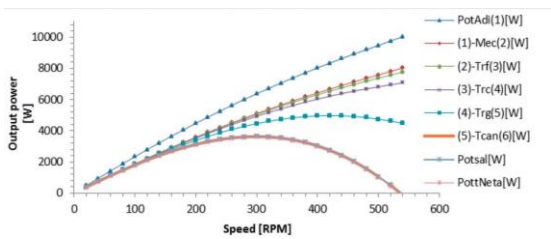

Source: by the author.

(1)= Output power adiabatic model (PotAdi).
(2)=(1) - mechanical losses (Mec).
(3)=(2) - friction losses in the cold exchanger (Trf).
(4)=(3) - friction losses in the hot exchanger (Trc).
(5)=(4) - friction losses in the regenerator (Trg).
(6)=(5) - loss by friction in the tubes of connectors of cold side (Tcan).

Output Power (Potsal) = (6) - loss by hysteresis in the compression and expansion chambers.

Net Output power (PottNeta)=Output Power (Potsal) - loss to outside pressure in the hot heat exchanger.

Proposal for improvement

The proposals for improvements in the Amazon engine are made by varying the geometry, component by component, until reaching a satisfactory relationship of the dead volume, efficiency and power generation. When making figures 7-10 the values of maximum power net found with changes in geometry are considered (length, number of tubes, diameter), regardless of engine velocity.

Hot heat exchanger. In this exchanger it´s necessary to strike a balance between heat transfer, dead volume, pressure losses in the outside of the exchanger and limitations in the manufacturing. The magnitude of dead volume presented in the collection of tubes (Figure 3) makes it important their elimination, but the placement of vertical tubes on the surface of the expansion chamber is from the manufacturing point of view, impossible. So the best choice is to place a horizontal tube in a vertical tube with equal diameter (tubes in U). The results of this improvement are presented in Figure 7. The maximum net power is achieved with an exhaust velocity of 6,5 m/s. The new configuration of the hot heat exchanger increases the net power in approximately 1.462 kW.

Figure 7. Variation of the maximum net power output, heat input and motor output, output temperature of exhaust and engine efficiency in terms of speed of the exhaust

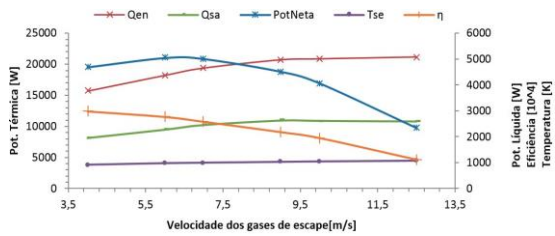

Source: by the author.

Regenerator. After previous changes, there were made changes to the length of the regenerator. Figure 8 shows the variations of maximum net power, heat input and engine output and engine efficiency with the length of the regenerator. The length of the regenerator with highest maximum net power (5.50 kW) is 5,6 cm. what it means to remove 6,4 cm of the current configuration. With an increase in net power output of 0,46 kW.

Figure 8. Variations of maximum power net, heat input and engine output and engine efficiency with the length of the regenerator

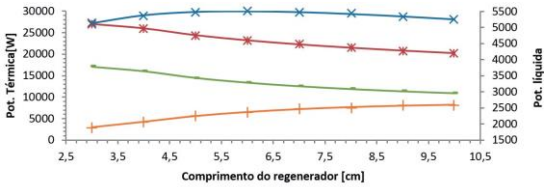

Source: by the author.

Tubes Connectors and Cold heat Exchanger. The connecting tubes (Figure 2) present a considerable friction loss due to their small cross sectional area. An increase in this area would reduce the loss of pressure drop, but also decrease the engine efficiency by increasing the dead volume. Furthermore, the area where you place the tubes (surface compression chamber) is shared with the compressor of the working fluid. Thus, the maximum number of pipes that can be put in is four. Figure 9 shows the variation of net maximum power and engine efficiency as a function of the diameter of the four tubes proposed. The maximum net power is achieved with a diameter of 2.4 cm in the four tubes.

Figure 9. Variation of net maximum power and engine efficiency as a function of diameter of the tubes connectors

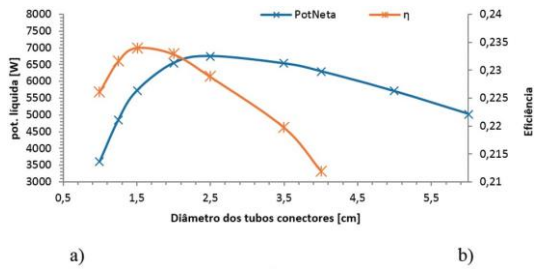

Source: by the author.

Despite having little friction losses in the cold heat exchanger, a variation in the number of tubes improves the dead volume without increasing the flow of cooling water. Figure 10 shows that with a number of 110 tubes maximum net power increases with 0,187 kW. The increase in the maximum net power of these two changes is 1.442 kW.

Figure 10. Variation of the maximum net power on function of the number of tubes of cold exchanger

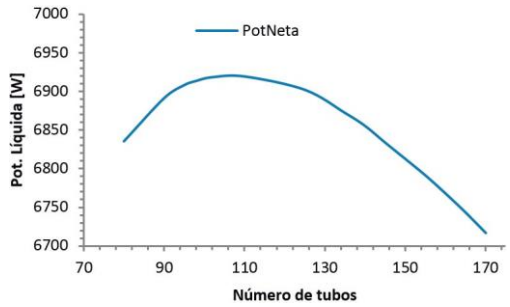

Source: by the author.

Final Result of Improved Amazon Engine

Figure 11 shows the characterization of losses and increase of net power with proposed changes. The additional losses in the cold heat exchanger, due to the decrease in the number of tubes are offset by the decrease in dead volume, the result being a gain in net power. Losses in the hot heat exchanger can be reduced by the elimination of sudden changes of the area due to the incorporation of horizontal tubes in the vertical tubes. In addition, the elimination of collector tubes diminishes much of the dead volume. The modification of the connecting tubes on the cold side increased the dead volume, but this is compensated with the reduction of friction losses. The power consumed by induced draft fan increases by the increase in pressure drop by the side of the exhaust gases due to new configuration of the hot heat exchanger.

Figure 11. Characterization of friction losses in the modified engine

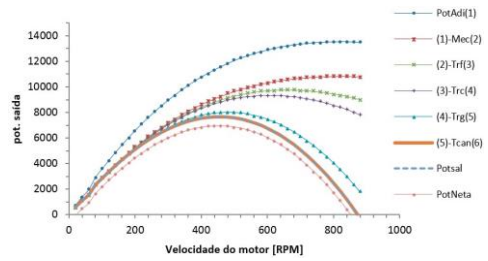

Source: by the author.

Figure 12 shows the temperature distribution in the heat exchanger (hot and cold), an increasing engine velocity causes a descend in

the temperature in the hot heat exchanger and an increase in the cold exchanger.

Figure 12. Temperature distribution in hot and cold heat exchangers to the current and modified engine

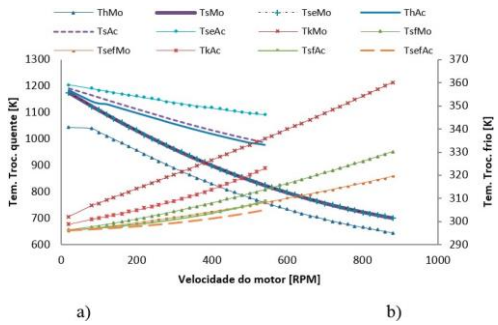

a) b)

Source: by the author.

Figure 13 shows the variation of losses in the engine when improvements are made component by component. The hot heat exchanger in the characterization of losses appears with small losses (Figure 6), but its potential for improvement is too high for the dead volume that it has originally. The connecting tubes, despite not being a primary component, have great potential for improvement, given its small cross-sectional area and quantity. The regenerator, despite having a considerable loss in its initial characterization (Figure 6), improves not as significant as the previous ones given its characteristics of porous cover.

Figure 13. Variation of loss by change in each of its components in the Amazon engine

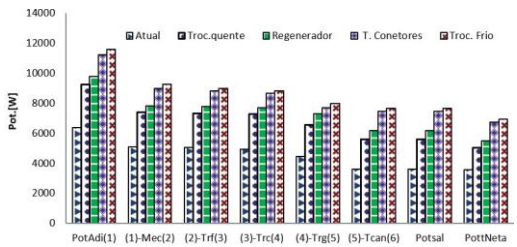

Source: by the author.

In Figure 14 is shown the influence of dead volume in the generation of power from the Amazon motor. The chart is done with the data supplied by the adiabatic model. Changes in motor decrease the total dead volume to 7330 cm^3, allowing a greater power generation and a greater pressure ratio.

Figure 14. Diagram of pressure - volume in the Stirling engine and modified current Amazon

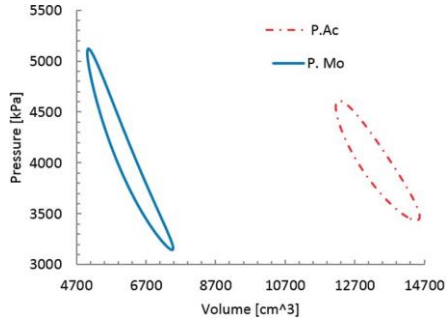

Source: by the author.

Conclusions

The integration of models of the heat exchangers, regenerator, accessories and induced draft fan in a second order adiabatic model, provide a valuable tool to improve efficiency and increase the potency of Stirling Amazon. On the other hand, the specificity with which it studies the hot heat exchanger allowed an optimization of this device, which is the most important and complex in Stirling engines supplied with the direct combustion of wood.

Because the PROSA software has had a hard work in testing and calibration, as well as greater consideration of losses, the results differ somewhat from those obtained by the model developed. However, the PROSA does not allow modeling of the geometric parameters of the hot heat exchanger or the variation of surface temperature of the heat exchangers depending on velocities of the external fluid (exhaust gases and water).

The low power generated by the Amazon Stirling engine at the time, is due mainly to large losses in the tubes connecting the cold side and dead volume of the collector tubes. These losses have decreased, in theory, with little change in the geometric parameters of the engine components. These changes are reflected in the reduction of dead volume to 7330 cm^3 and an increase in output power of 3,3 kW, reaching an output power of 6,95 kW at 460 rpm. this value of power generated does not reach the originally projected, but is reasonable because in the initial project the power supplied to the induced draft fan was not taken into account. For the modified engine this value, with velocity of exhaust optima, is 0,72

References

Aliabadi, A. A., Thomson, M. J., Wallace, J. S., Tzanetakis, T., Lamont, W. & Di Carlo, J. (2009). Efficiency and Emissions Measurement of a Stirling-Engine-Based Residential Microcogeneration System Run on Diesel and Biodiesel. *Energy & Fuels*, 23, 1032 - 1039.

Bergman, T. L., Lavine, A. S., Incropera, F. P. & DeWitt, D. P. (1996). F*undamentals of Heat and Mass Transfer*. 4ta ed. Nueva York: Pearson.

Bridgwater, A. (2003). Renewable fuels and chemicals by thermal processing of biomass. *Chemical Engineering Journal*, 91, 87 - 102.

Cullen, B. & McGovern, J. (2010). Development of a theoretical decoupled Stirling cycle engine. *Simulation Modelling Practice and Theory*, 19, 4, 1227 - 1234.

Hargreaves, C. (1991). *The Philips Stirling Engine*. Ámsterdam: Elsevier Publishing Company.

Hausen, H. (1929). Über die Theorie des Waermeaustausch in Regeneratoren. *Zeitschrift des Vereins deutscher Ingenieure*, 73, 3, 173 - 200.

Kuosa, M., Kaikko, J. & Koskelainen, L. (2007). The impact of heat exchanger fouling on the optimum operation and maintenance of the Stirling engine. *Applied Thermal Engineering*, 27, 1671 - 1676.

Lundqvist, G. (1993). *Stirling cycle heat pumps and refrigerators* [doctoral thesis]. Suecia, Estocolmo, Institutionen för Mekanisk. The Royal Institute of Technology.

Martini, W. (1983). *Stirling Engine Design Manual*. United States: NASA, U. S., Department of Energy.

Organ, A. (1997). *The Regenerator and the Stirling Engine*. Nueva York: John Wiley & Sons.

Podesser, E. (1999). Electricity Production in Rural Villages with a Biomass Stirling Engine. *Renewable Energy*, *1*6, 1049 - 1052.

Thombare, D. G. & Verma, S. K. (2008). Technological development in the Stirling cycle engines. *Renewable and Sustainable Energy Reviews*, 12, 1 - 38.

Timoumi, Y., Tliliun, I. & Nasrallahun, B. (2008). Design and performance optimization of GPU-3 Stirling engines. *Energy*, 33, 1100 - 1114.

Urieli, I. & Berchowitz, D. (1984). *Stirling cycle engine analysis*. Bristol: Adam Hilger Ltd.

Walker, G. (1980). *Stirling Engines*. Oxford: Clarendon Press.

Wilke, H. & Silva, E. (2004). Desenvolvimento de um módulo combustor biomassa-motor stirling aplicado a sistemas de geração isolada e baseados em gerador de indução. In Anais do *5º Encontro de Energia no Meio Rural*. Campinas (SP).